





## Dynamic clustering of active rings

Ligesh Theeyancheri <sup>1</sup>, Subhasish Chaki <sup>1,2</sup>, Tapomoy Bhattacharjee <sup>3,\*</sup> and Rajarshi Chakrabarti <sup>1,†</sup>

<sup>1</sup>*Department of Chemistry, Indian Institute of Technology Bombay, Mumbai 400076, India*

<sup>2</sup>*Institut für Theoretische Physik II - Soft Matter, Heinrich-Heine-Universität Düsseldorf, Universitätsstraße 1, D-40225 Düsseldorf, Germany*

<sup>3</sup>*National Centre for Biological Sciences, Tata Institute of Fundamental Research, Bangalore 560065, India*



(Received 16 November 2023; accepted 19 January 2024; published 22 February 2024)

A collection of rings made of active Brownian particles (ABPs) for different packing fractions and activities is investigated using computer simulations. We show that active rings display an emergent dynamic clustering instead of the conventional motility-induced phase separation (MIPS) as in the case of collection of ABPs. Surprisingly, increasing packing fraction of rings exhibits a nonmonotonicity in the dynamics due to the formation of a large number of small clusters. The conformational fluctuations of the polymers suppress the usual MIPS exhibited by ABPs. Our findings demonstrate how the motion of a collection of rings is influenced by the interplay of activity, topology, and connectivity.

DOI: [10.1103/PhysRevResearch.6.L012038](https://doi.org/10.1103/PhysRevResearch.6.L012038)

Active agents such as bacteria [1], colloids locally driven by chemical reactions [2–4], temperature gradient [5], or by some other means operate far from thermal equilibrium as they use an internal source of energy to generate directed motion [6] and break the time-reversal symmetry [7]. Biological examples of collection of active agents include suspensions of motile microorganisms, collective organization of cells in living tissues, and flocks of birds [8–15]. Synthetic examples include vibrated granular monolayers [16] and suspension of phoretic colloidal particles [17], etc. Collectively these active units show interesting behavior such as swarming [9,13], flocking [18], and nonequilibrium ordering [19].

Another interesting phenomena that has been observed for a collection of active particles is motility-induced phase separation (MIPS) where the system phase separates into two distinct phases, dilute and dense [11,20]. This is intriguing as it is purely due to persistent active motion in the absence of any sort of attractive interaction [21,22]. How the phase behavior is affected by the polydisperse nature of the active particles [11,12,20], and the softness of interactions [23,24] have also been studied. The majority of the studies on MIPS have focused on active colloids that lack conformational fluctuations of the system. Recent works on complex active systems, such as active polymers, have shown rich and counterintuitive structural and dynamical properties [25–42]. The coupling of activity and conformations of polymers give rise to novel phenomena, such as an activity-induced polymer

collapse or swelling and a transition from a trapped state to escape in porous media [43–45]. This illustrates that the understanding of active processes in the collection of polymers may be essential to designing new classes of active soft materials.

Our goal in this work is to study the dynamics and structure of a collection of self-propelled disks (in two dimensions) connected by springs to form a ring made of active disks. In the absence of these springs, the system undergoes MIPS depending on density and activity [11,20]. But will these active rings also separate into a dense and dilute phase, in other words, undergo MIPS? This remains unexplored to the best of our knowledge. However, if the system does not show MIPS, what is the underlying reason, and if it does, then how does it differ from the usual MIPS as shown by ABPs? This is an important question to ask, as polymers undergoing phase separation due to some sort of motility has been a topic of research in recent years [37,46–48]. This is pertinent in the context of chromatin [46,47], malaria parasites [48], etc. For example, the chromatin phase separates into dense and dilute phases [46,47]. The activity in that case, however, was introduced by putting a fraction of consecutive monomers on a polymer to stronger thermal fluctuations than the rest, i.e., by making them effectively hotter.

Our simulations with active rings show that the dynamics is strikingly different for rings compared to that of ABPs. While ABPs undergo MIPS, rings made of ABPs do not, instead formation of intermittent unstable clusters is observed. These clusters are dynamic as they form and disintegrate continuously. Further analyses of cluster size and numbers reveal that increasing activity (active force on each monomer) facilitates the formation of a large number of smaller clusters. Notably, faster dynamics of this collection of active rings emerge at higher packing fractions due to the combined effects of the activity-induced shape deformation and dynamic clustering of the rings. The formation of highly motile and dense small

\*tapa@ncbs.res.in

†rajarshi@chem.iitb.ac.in

Published by the American Physical Society under the terms of the [Creative Commons Attribution 4.0 International license](https://creativecommons.org/licenses/by/4.0/). Further distribution of this work must maintain attribution to the author(s) and the published article's title, journal citation, and DOI.

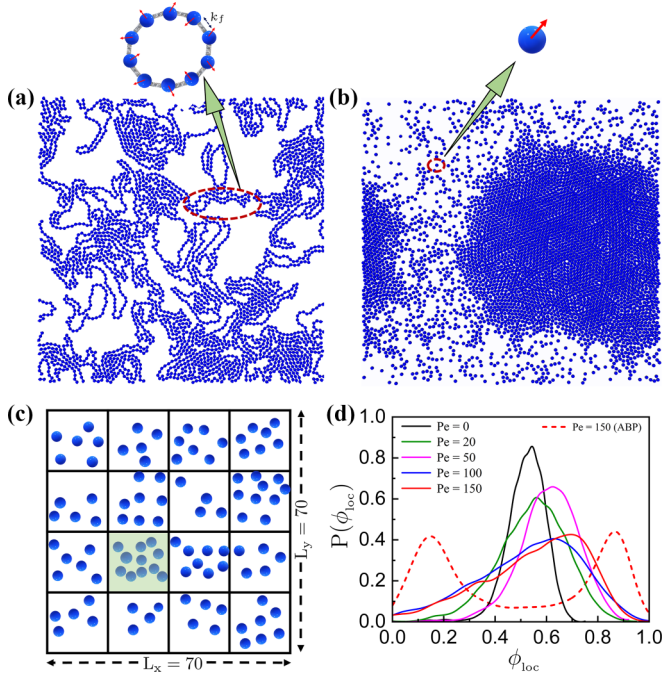


FIG. 1. Snapshots of a collection of (a) rings made of ABPs and (b) ABPs for  $Pe = 150$  at  $\phi = 0.48$ . The red arrows represent the instantaneous directions of active force. A schematic sketch of a ring and an ABP is shown. The snapshots display the emergent dynamic clustering of active rings and motility-induced phase separation of ABPs for  $Pe = 150$  at the same  $\phi = 0.48$ . (c) Schematic showing the method used for local density calculation, where  $\phi_{loc}$  is the number of particles in the shaded region divided by the area of that region. (d)  $P(\phi_{loc})$  vs  $\phi_{loc}$  for different  $Pe$  at  $\phi = 0.48$ . The dashed line represents the curve for ABPs of the same  $\phi$ .

clusters at higher  $\phi$  is due to the interplay of activity, deformation, and stress governing events in the system. Our model demonstrates the emergence of a fascinating dynamic clustering of active rings made of ABPs, which is different from the conventional MIPS behavior exhibited by ABPs.

We model the rings as a sequence of  $n$  number of ABPs of diameter  $\sigma$  at positions  $r_i$  ( $i = 1, 2, \dots, n$ ) that are connected by  $n$  finitely extensible springs [Fig. 1(a)]. In contrast to existing efforts of simulating active dynamics of ring polymers, our model does not impose any external polarity [34] or tangential activity [49]. Rather, it captures the emergent properties of the ensemble of active rings with random motility and therefore is quite unique. We pack  $N$  number of such rings in a two-dimensional (2D) square box of length  $L_x = L_y = 70\sigma$  to achieve different packing fractions,  $\phi$ . The motion of each particle (monomer) is governed by the overdamped Langevin equation:

$$\gamma \frac{d\mathbf{r}_i}{dt} = - \sum_j \nabla V(\mathbf{r}_i - \mathbf{r}_j) + \mathbf{f}_i(t) + \mathbf{F}_{a,i}(t), \quad (1)$$

where the drag force,  $\gamma \frac{d\mathbf{r}_i}{dt}$  is the velocity of  $i$ th monomer times the friction coefficient  $\gamma$ , and the total interaction potential  $V(r) = V_{FENE} + V_{BEND} + V_{WCA}$  consists of bond, bending, and excluded volume contributions (see Supplemental Material (SM) [50] for details). Thermal fluctuations are

captured by the Gaussian random force  $f_i(t)$ , which must satisfy the fluctuation-dissipation theorem. The activity is modeled as a propulsive force  $F_a \mathbf{n}(\theta_i)$  on each monomer where  $F_a$  represents the amplitude of active force with orientation specified by the unit vector  $\mathbf{n}(\theta_i)$  evolves according to thermal rotational diffusion [6] (see SM for details [50]). In our simulation,  $\sigma$ ,  $k_B T$ , and  $\tau = \frac{\sigma^2 \gamma}{k_B T}$  set the unit of length, energy, and time scales, respectively. We express the activity in terms of a dimensionless quantity, Péclet number as  $Pe = \frac{F_a \sigma}{k_B T}$  [43,45].

We first simulate ABPs in two dimensions for different activities for a given packing fraction,  $\phi = 0.48$ , where  $\phi = \frac{N n \pi \sigma^2}{4 L_x \times L_y}$ , where  $N$  is the number of rings and  $n$  is the number of monomers with diameter  $\sigma$  per rings. Our results show that ABPs undergo nonequilibrium clustering similar to other model active systems. We establish that this clustering is indeed activity-driven phase separation by estimating the local density,  $\phi_{loc}$  for different  $Pe$  [Fig. 1(d)]. For lower activities, the system behaves like a fluid, and  $P(\phi_{loc})$  has a single peak around the bulk density, but for higher activities, ABPs start to form clusters and the local density distribution changes from unimodal to bimodal [11]. This signifies the phase separation and existence of two distinct phases in the system.

Next, we investigate the behavior of an ensemble of active Brownian rings at the same  $\phi$  as ABPs to see how the conventional MIPS-like behavior is influenced by connecting the ABPs together to form the rings. For the passive rings, the peak of the  $P(\phi_{loc})$  occurs at  $\phi_{loc} = 0.48$ , i.e., at the bulk density  $\phi$ . In the presence of activity,  $P(\phi_{loc})$  broadens with peak shifted to higher density at very high  $Pe$  [Fig. 1(d)]. Even for  $Pe = 150$ , where ABPs show MIPS, active rings do not exhibit two distinct phases. This denotes a dynamic clustering of active rings as a function of increasing  $Pe$ . Active rings form low and highly dense states (Fig. S2 [50]), and these states are not stable as the cluster degradation happens, which is more pronounced with increasing  $Pe$  (Movie\_S1-S2 [50]). However, the center of mass of the rings shows enhanced dynamics with intermediate superdiffusion as a function of increasing  $Pe$  (Fig. S3 [50]).

To further characterize the nature of the dynamic clustering of active rings, we compute the probability distribution of the number of clusters  $N_{clusters}$ ,  $P(N_{clusters})$  and size of the clusters  $S_{clusters}$ ,  $P(S_{clusters})$  formed for different  $Pe$ . If a minimum of four particles of the same or different rings are closely spaced within a cutoff distance of  $1.12\sigma$ , then we defined them as a cluster. We observe a broader density profile, and the peak shifts towards the larger value for  $P(N_{clusters})$  with increasing  $Pe$ , while a reverse trend can be seen in  $P(S_{clusters})$ , where the distribution become narrower and peaks shift to lower values of  $S_{clusters}$  (Fig. 2). This indicates the emergence of multiple dynamic clusters, and they continuously coalesce, split, and decay but never merge and grow into a stable dense phase like ABPs.

To elucidate the dynamic clustering, we consider the conformations and shape deformation of the active rings for different  $Pe$  (Fig. S4 [50]). We generate the probability distribution of the radius of gyration  $R_g$ ,  $P(R_g)$ .  $P(R_g)$  demonstrates the activity-induced collapse of the rings as the most probable  $R_g$  shifts to smaller values with increasing  $Pe$  (Fig. S4(a) [50]).

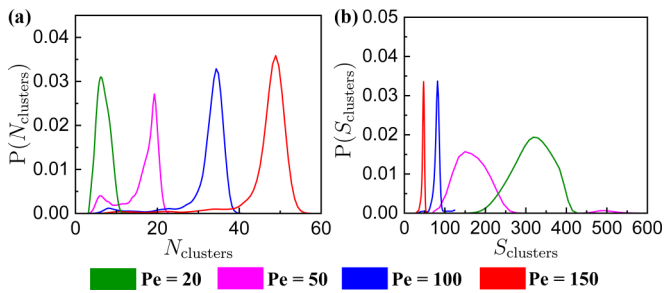


FIG. 2. (a)  $P(N_{\text{clusters}})$  vs  $N_{\text{clusters}}$  and (b)  $P(S_{\text{clusters}})$  vs  $S_{\text{clusters}}$  for different  $Pe$  at  $\phi = 0.48$ .

We also calculate the asphericity parameter,  $A = \frac{(\lambda_2 - \lambda_1)^2}{(\lambda_1 + \lambda_2)^2}$ , where  $\lambda_1$  and  $\lambda_2$  are the eigenvalues of the gyration tensor.  $P(A)$  indicates that the extent of the ring deformation from the circular one also increases with the increase in  $Pe$ . Active rings undergo moderate deformation at lower  $Pe$  followed by more stronger deformation within a small fraction of rings at high  $Pe$  (Fig. S4(b) [50]). The rings are coming closer in the cluster due to activity, which leads to the shape deformation and the collapse of the rings.

Subsequently, we examine how deformation and stress are distributed within the system in Fig. 3, where we plot the maximum eigenvalues of stress tensor ( $\Sigma^{\text{Max}}$ ) against maximum eigenvalues of gyration tensor ( $R_g^{\text{Max}}$ ). Figure 3 displays that the eigenvalues of the stress and the gyration tensor are correlated so that the stress increases to a large extent, rings deform and shrink with increasing  $Pe$ . The negative values of the stress indicate that this is of a compressive nature. For passive rings, the stress contribution is from the bonded interactions as there is no clustering [Fig. 3(a)]. On the other hand, active rings display an enhancement in stress due to the deformation-induced shrinking with increasing  $Pe$ .

The results derived so far demonstrate how the motion of a collection of active rings deviates from the conventional behavior exhibited by ABPs as a function of  $Pe$ . Now, we examine how the packing fraction ( $\phi$ ) influences the dynamics and clustering of active rings. We compute the center of mass mean-square displacement,  $\langle \Delta r_c^2(\tau) \rangle$  of the rings with increasing  $\phi$  [Fig. 4(a)]. For the passive rings, the dynamics becomes slower with increasing  $\phi$  and consequently,  $\langle \Delta r_c^2(\tau) \rangle$  show a monotonic decrease with  $\phi$ . Conversely, we notice a nonmonotonic behavior in the dynamics of active rings where  $\langle \Delta r_c^2(\tau) \rangle$  first decreases up to an intermediate  $\phi$

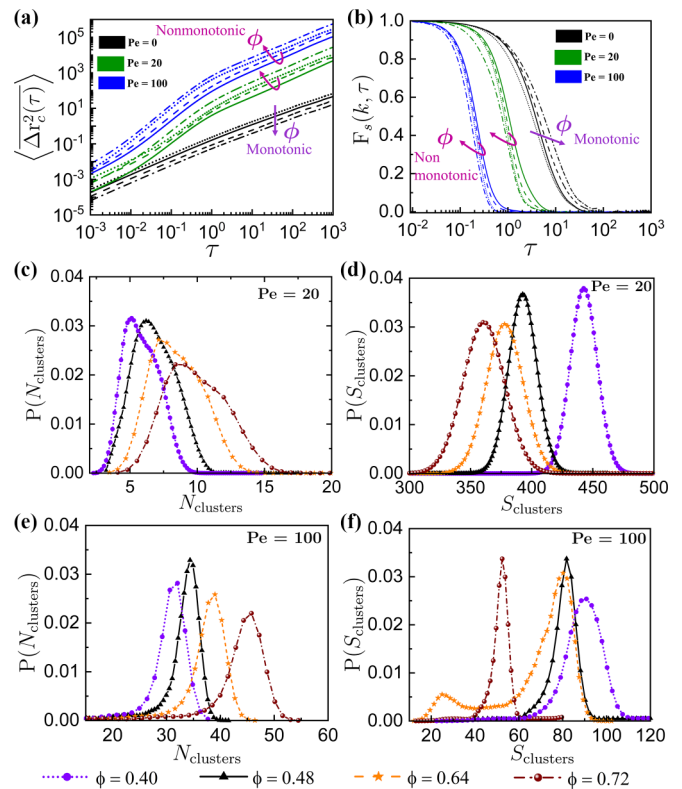


FIG. 4. (a) Log-log plot of  $\langle \Delta r_c^2(\tau) \rangle$ , (b) log-linear plot of  $F_s(k, \tau)$  vs  $\tau$  for  $Pe = 0$ ,  $Pe = 20$ , and  $Pe = 100$  for  $\phi = 0.40$  (dotted),  $\phi = 0.48$  (solid),  $\phi = 0.64$  (dashed), and  $\phi = 0.72$  (dash-dotted). The magenta and violet colored arrows indicate the nonmonotonic and monotonic behavior in the dynamics of active rings as a function of increasing  $\phi$ .  $P(N_{\text{clusters}})$  vs  $N_{\text{clusters}}$  and  $P(S_{\text{clusters}})$  vs  $S_{\text{clusters}}$  for  $Pe = 20$  (c and d), and  $Pe = 100$  (e and f) for different  $\phi$ .

then increases upon further increasing  $\phi$ . The nonmonotonic behavior observed for active rings is directly correlated to the breakdown of the clusters in smaller ones at large  $\phi$ . The cluster number and size for  $Pe = 20$  [Figs. 4(c), 4(d)] and  $Pe = 100$  [Figs. 4(e), 4(f)] display formation of a large number of smaller clusters with increasing  $\phi$  (Movie\_S2-S4 [50]). The peaks of  $P(N_{\text{clusters}})$  shift to higher values of  $N_{\text{clusters}}$ , while the most probable values of  $P(S_{\text{clusters}})$  shift to smaller values of  $S_{\text{clusters}}$  as function of increasing  $\phi$ . This behavior is more pronounced at higher  $Pe$  as the cluster formed are much smaller

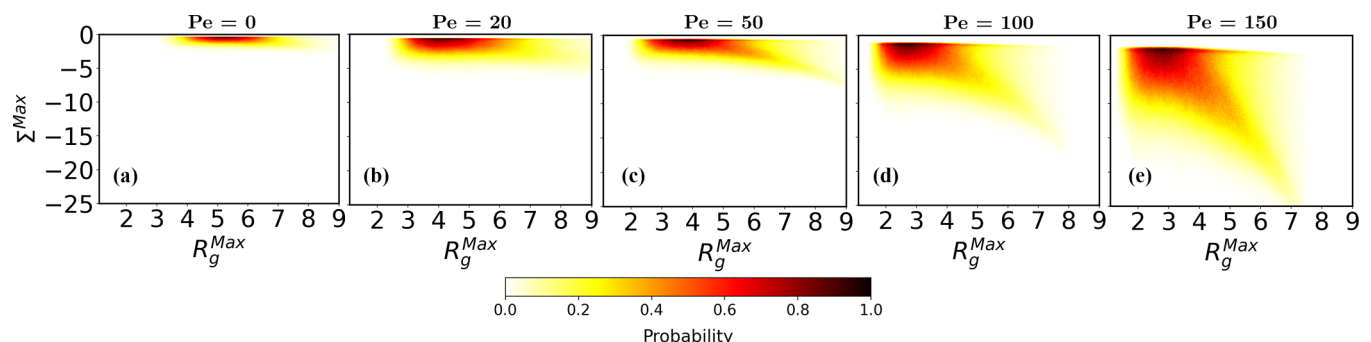


FIG. 3. 2D probability of  $R_g^{\text{Max}}$  and that of  $\Sigma^{\text{Max}}$  for (a)  $Pe = 0$ , (b)  $Pe = 20$ , (c)  $Pe = 50$ , (d)  $Pe = 100$ , and (e)  $Pe = 150$  at  $\phi = 0.48$ .

in size compared to lower  $Pe$  for all  $\phi$ . This signifies the formation of highly motile smaller and dense clusters at higher  $\phi$  (Fig. S5 [50]), which in turn results in faster motion of the active rings. We also report the self-intermediate scattering functions  $F_s(k, \tau)$  for  $k$  corresponds to the first peak of the radial distribution functions for different  $\phi$ .  $F_s(k, \tau)$  decays slowly followed by a fast decay with increasing  $\phi$  while the associated relaxation time  $\tau_d$  first increases and then decreases with increasing  $\phi$  (Fig. S6 [50]), which further confirms the nonmonotonic behavior observed for active rings [Fig. 4(b)].

Our *in silico* model identifies how the motion of an ensemble of active rings is regulated by the crucial structural and dynamic factors that control their motion. A dense suspension of ABPs separates into two distinct phases as seen in the local density plot [Fig. 1(d)]. But the phenomenon is quite different when these ABPs are connected to form rings. This system does not show MIPS. Instead, an emergent dynamic clustering of rings is observed. The presence of springs prevents the system from undergoing MIPS. The interplay between activity (motility), topology, and crowding drives the system to form intermittent clusters but never allows it to grow into a large dense phase/cluster. Our simulations exhibit that the translational motion of the center of mass of the rings is enhanced by the activity for a given  $\phi$ . Interestingly, the behavior of the system changes drastically with increasing  $\phi$ . The translational dynamics of the system becomes

faster at higher  $\phi$  and also displays an emergent dynamic clustering of active rings. The size and number of clusters largely depend on the magnitude of  $Pe$  and  $\phi$ . At higher  $\phi$ , dynamic clustering leads to the formation of highly motile smaller and dense clusters. Our model finds that the dynamic clustering is different from MIPS because the stress building in the dynamic clusters by the activity-induced deformation (Figs. S7–S8 [50]) followed by the stress releasing via cluster degradation as the monomers are connected by springs, which suppresses the formation of stable dense and dilute regions of active rings. The deformation of rings and activity-assisted stress governing events lead to the emergence of distinctive dynamic clustering of active rings, which is completely absent in the passive case [Fig. 3(a)]. We believe our study, in general will be insightful in understanding the structure and dynamics of densely packed deformable objects driven by motility.

L.T. thanks UGC for a fellowship and IIT Bombay for the institute postdoctoral fellowship. S.C. thanks DST Inspire for a fellowship. R.C. acknowledges SERB for funding (Project No. MTR/2020/000230 under MATRICS scheme). T.B. acknowledges NCBS-TIFR for research funding. L.T. thanks Pooja Nanavare for the help and proofreading. The authors thank K. Kumar for the initial discussions and for performing some trial simulations.

- 
- [1] X.-L. Wu and A. Libchaber, Particle diffusion in a quasi-two-dimensional bacterial bath, *Phys. Rev. Lett.* **84**, 3017 (2000).
- [2] P. Illien, R. Golestanian, and A. Sen, ‘Fuelled’ motion: phoretic motility and collective behaviour of active colloids, *Chem. Soc. Rev.* **46**, 5508 (2017).
- [3] S. Samin and R. van Roij, Self-propulsion mechanism of active janus particles in near-critical binary mixtures, *Phys. Rev. Lett.* **115**, 188305 (2015).
- [4] I. Buttinoni, G. Volpe, F. Kümmel, G. Volpe, and C. Bechinger, Active brownian motion tunable by light, *J. Phys.: Condens. Matter* **24**, 284129 (2012).
- [5] H.-R. Jiang, N. Yoshinaga, and M. Sano, Active motion of a Janus particle by self-thermophoresis in a defocused laser beam, *Phys. Rev. Lett.* **105**, 268302 (2010).
- [6] C. Bechinger, R. Di Leonardo, H. Löwen, C. Reichhardt, G. Volpe, and G. Volpe, Active particles in complex and crowded environments, *Rev. Mod. Phys.* **88**, 045006 (2016).
- [7] J. O’Byrne, Y. Kafri, J. Tailleur, and F. van Wijland, Time irreversibility in active matter, from micro to macro, *Nature Rev. Phys.* **4**, 167 (2022).
- [8] F. Peruani, A. Deutsch, and M. Bär, Nonequilibrium clustering of self-propelled rods, *Phys. Rev. E* **74**, 030904(R) (2006).
- [9] S. Ramaswamy, R. A. Simha, and J. Toner, Active nematics on a substrate: Giant number fluctuations and long-time tails, *Europhys. Lett.* **62**, 196 (2003).
- [10] A. Gopinath, M. F. Hagan, M. C. Marchetti, and A. Baskaran, Dynamical self-regulation in self-propelled particle flows, *Phys. Rev. E* **85**, 061903 (2012).
- [11] G. S. Redner, M. F. Hagan, and A. Baskaran, Structure and dynamics of a phase-separating active colloidal fluid, *Phys. Rev. Lett.* **110**, 055701 (2013).
- [12] T. Vicsek and A. Zafeiris, Collective motion, *Phys. Rep.* **517**, 71 (2012).
- [13] D. Grober, I. Palaia, M. C. Uçar, E. Hannezo, A. Šarić, and J. Palacci, Unconventional colloidal aggregation in chiral bacterial baths, *Nature Phys.* **19**, 1680 (2023).
- [14] S. Garcia, E. Hannezo, J. Elgeti, J.-F. Joanny, P. Silberzan, and N. S. Gov, Physics of active jamming during collective cellular motion in a monolayer, *Proc. Natl. Acad. Sci. USA* **112**, 15314 (2015).
- [15] A. Hopkins, B. Loewe, M. Chiang, D. Marenduzzo, and M. C. Marchetti, Motility induced phase separation of deformable cells, *Soft Matter* **19**, 8172 (2023).
- [16] J. Deseigne, O. Dauchot, and H. Chaté, Collective motion of vibrated polar disks, *Phys. Rev. Lett.* **105**, 098001 (2010).
- [17] F. Ginot, I. Theurkauff, D. Levis, C. Ybert, L. Bocquet, L. Berthier, and C. Cottin-Bizonne, Nonequilibrium equation of state in suspensions of active colloids, *Phys. Rev. X* **5**, 011004 (2015).
- [18] S. Ramaswamy, The mechanics and statistics of active matter, *Annu. Rev. Condens. Matter Phys.* **1**, 323 (2010).
- [19] K. R. Prathyusha, S. Henkes, and R. Sknepnek, Dynamically generated patterns in dense suspensions of active filaments, *Phys. Rev. E* **97**, 022606 (2018).
- [20] M. E. Cates and J. Tailleur, Motility-induced phase separation, *Annu. Rev. Condens. Matter Phys.* **6**, 219 (2015).
- [21] T. Speck, J. Bialké, A. M. Menzel, and H. Löwen, Effective Cahn-Hilliard equation for the phase separation of active brownian particles, *Phys. Rev. Lett.* **112**, 218304 (2014).
- [22] U. Basu, S. N. Majumdar, A. Rosso, and G. Schehr, Active brownian motion in two dimensions, *Phys. Rev. E* **98**, 062121 (2018).

- [23] S. De Karmakar and R. Ganesh, Motility-induced phase separation of self-propelled soft inertial disks, *Soft Matter* **18**, 7301 (2022).
- [24] D. Martin, J. O'Byrne, M. E. Cates, É. Fodor, C. Nardini, J. Tailleur, and F. van Wijland, Statistical mechanics of active Ornstein-Uhlenbeck particles, *Phys. Rev. E* **103**, 032607 (2021).
- [25] T. Eisenstecken, G. Gompper, and R. G. Winkler, Conformational properties of active semiflexible polymers, *Polymers* **8**, 304 (2016).
- [26] S. M. Mousavi, G. Gompper, and R. G. Winkler, Active brownian ring polymers, *J. Chem. Phys.* **150**, 064913 (2019).
- [27] A. Ghosh and N. Gov, Dynamics of active semiflexible polymers, *Biophys. J.* **107**, 1065 (2014).
- [28] T. B. Liverpool, A. C. Maggs, and A. Ajdari, Viscoelasticity of solutions of motile polymers, *Phys. Rev. Lett.* **86**, 4171 (2001).
- [29] Y. Roichman, D. G. Grier, and G. Zaslavsky, Anomalous collective dynamics in optically driven colloidal rings, *Phys. Rev. E* **75**, 020401(R) (2007).
- [30] Ö. Duman, R. E. Isele-Holder, J. Elgeti, and G. Gompper, Collective dynamics of self-propelled semiflexible filaments, *Soft Matter* **14**, 4483 (2018).
- [31] A. Rosa and R. Everaers, Ring polymers in the melt state: the physics of crumpling, *Phys. Rev. Lett.* **112**, 118302 (2014).
- [32] N. Nahali and A. Rosa, Density effects in entangled solutions of linear and ring polymers, *J. Phys.: Condens. Matter* **28**, 065101 (2016).
- [33] J. H. Choi, T. Kwon, and B. J. Sung, Relative chain flexibility determines the spatial arrangement and the diffusion of a single ring chain in linear chain films, *Macromolecules* **54**, 11008 (2021).
- [34] H. Wen, Y. Zhu, C. Peng, P. B. Sunil Kumar, and M. Laradji, Collective vortical motion and vorticity reversals of self-propelled particles on circularly patterned substrates, *Phys. Rev. E* **107**, 024606 (2023).
- [35] K. Goswami, S. Chaki, and R. Chakrabarti, Reconfiguration, swelling and tagged monomer dynamics of a single polymer chain in gaussian and non-gaussian active baths, *J. Phys. A: Math. Theor.* **55**, 423002 (2022).
- [36] N. Gnan and E. Zaccarelli, The microscopic role of deformation in the dynamics of soft colloids, *Nature Phys.* **15**, 683 (2019).
- [37] J. Smrek, I. Chubak, C. N. Likos, and K. Kremer, Active topological glass, *Nature Commun.* **11**, 26 (2020).
- [38] J. Chattopadhyay, S. Ramaswamy, C. Dasgupta, and P. K. Maiti, Two-temperature activity induces liquid-crystal phases inaccessible in equilibrium, *Phys. Rev. E* **107**, 024701 (2023).
- [39] N. Venkatarreddy, J. Mandal, and P. K. Maiti, Effect of confinement and topology: 2-TIPS vs. MIPS, *Soft Matter* **19**, 8561 (2023).
- [40] J. Huang, H. Levine, and D. Bi, Bridging the gap between collective motility and epithelial–mesenchymal transitions through the active finite voronoi model, *Soft Matter* **19**, 9389 (2023).
- [41] J. P. Miranda, E. Locatelli, and C. Valeriani, Self-organized states from solutions of active ring polymers in bulk and under confinement, *J. Chem. Theory Comput.* (2023), doi:10.1021/acs.jctc.3c00818.
- [42] E. Locatelli, V. Bianco, and P. Malmaretti, Activity-induced collapse and arrest of active polymer rings, *Phys. Rev. Lett.* **126**, 097801 (2021).
- [43] L. Theeyancheri, S. Chaki, T. Bhattacharjee, and R. Chakrabarti, Migration of active rings in porous media, *Phys. Rev. E* **106**, 014504 (2022).
- [44] P. Chopra, D. Quint, A. Gopinathan, and B. Liu, Geometric effects induce anomalous size-dependent active transport in structured environments, *Phys. Rev. Fluids* **7**, L071101 (2022).
- [45] L. Theeyancheri, S. Chaki, T. Bhattacharjee, and R. Chakrabarti, Active dynamics of linear chains and rings in porous media, *J. Chem. Phys.* **159**, 014902 (2023).
- [46] A. Agrawal, N. Ganai, S. Sengupta, and G. I. Menon, Chromatin as active matter, *J. Stat. Mech.* (2017) 014001.
- [47] G. Shi, L. Liu, C. Hyeon, and D. Thirumalai, Interphase human chromosome exhibits out of equilibrium glassy dynamics, *Nature Commun.* **9**, 3161 (2018).
- [48] P. Patra, K. Beyer, A. Jaiswal, A. Battista, K. Rohr, F. Frischknecht, and U. S. Schwarz, Collective migration reveals mechanical flexibility of malaria parasites, *Nature Phys.* **18**, 586 (2022).
- [49] V. Bianco, E. Locatelli, and P. Malmaretti, Globulelike conformation and enhanced diffusion of active polymers, *Phys. Rev. Lett.* **121**, 217802 (2018).
- [50] See Supplemental Material at <http://link.aps.org/supplemental/10.1103/PhysRevResearch.6.L012038> for model and simulation details, intermediate scattering function, gyration tensor analysis, stress tensor analysis, additional plots, and Supplemental Movie descriptions discussed in the paper.